(13) Luongo, J. P. *J. Polym. Sci., Part A-2* **1972**, *10*, 1119.
(14) Dvey-Aharon, H.; Taylor, P. L.; Hopfinger, A. J. *J. Appl. Phys.* **1980**, *51*, 5184.
(15) Banik, N. C.; Taylor, P. L.; Hopfinger, A. J. *Appl. Phys. Lett.* **1980**, *37*, 49.
(16) Kobayashi, M.; Tashiro, K.; Tadokoro, H. *Macromolecules* **1975**, *8*, 158.
(17) Cortili, G.; Zerbi, G. *Spectrochim. Acta, Part A* **1967**, *23A*, 2216.
(18) Naegele, D.; Yoon, D. Y. *Appl. Phys. Lett.* **1978**, *33*, 132.
(19) Barker, R. E., Jr.; Campbell, K. W.; Huang, C. C. *Bull. Am. Phys. Soc.* **1985**, *30* (3), 491.
(20) Stein, R. S., to be published.
(21) Lu, F. J.; Hsu, S. L. *Polymer* **1985**, *25*, 1247.
(22) Lu, F. J.; Waldman, D. A.; Hsu, S. L. *J. Polym. Sci., Polym. Phys. Ed.* **1984**, *22*, 827.
(23) Takashasi, T.; Date, M.; Fukada, E. *Ferroelectrics* **1981**, *32*, 73.
(24) Bachmann, M. A.; Gordon, W. L.; Koenig, J. L.; Lando, J. B. *J. Appl. Phys.* **1978**, *50*, 6106.
(25) Yang, D. N.; Thomas, E. L. *J. Mat. Sci. Lett.*, in press.
(26) Furukawa, T.; Date, M.; Fukada, E. *J. Appl. Phys.* **1980**, *51*, 1135.
(27) Murayama, N.; Oikawa, T.; Katto, T.; Nakamura, K. *J. Polym. Sci., Polym. Phys. Ed.* **1975**, *13*, 1033.
(28) Blevin, W. R. *Appl. Phys. Lett.* **1977**, *31*, 6.
(29) Scheinbeim, J. I.; Yoon, C. H.; Pae, K. D.; Newman, B. A. *J. Polym. Sci., Polym. Phys. Ed.* **1980**, *18*, 2271.
(30) Sussner, H.; Dransfeld, K. *J. Polym. Sci., Polym. Phys. Ed.* **1978**, *16*, 529.
(31) Shuford, R. J.; Wilde, A. F.; Ricca, J. J.; Thomas, G. R. *Polym. Eng. Sci.* **1976**, *16*, 25.
(32) Naegele, D.; Yoon, D. Y.; Broadhurst, M. G. *Macromolecules* **1978**, *11*, 1297.
(33) Lovinger, A. J. *Macromolecules* **1981**, *14*, 225.
(34) Lovinger, A. J. *J. Appl. Phys.* **1981**, *52*, 5934.
(35) Takahashi, Y.; Tadokoro, H. *Macromolecules* **1980**, *13*, 1316.
(36) Farmer, B. L.; Hopfinger, A. J.; Lando, J. B. *J. Appl. Phys.* **1972**, *43*, 4293.

Conformational Change, Chain Orientation, and Crystallinity in Poly(ethylene terephthalate) Yarns: Raman Spectroscopic Study

Bernard J. Bulkin,* Menachem Lewin,† and Frank J. DeBlase

Department of Chemistry and Polymer Research Institute, Polytechnic Institute of New York, Brooklyn, New York 11201. *Received February 27, 1985*

ABSTRACT: A Raman spectroscopic study of five fibers of poly(ethylene terephthalate) is presented. These fibers are produced by annealing an original fiber under different temperatures and shrinkage conditions. The result is five spectra that are different in many ways. Included are results in the low-frequency region of the spectrum. Analysis of these results is approached in terms of three distinct types of events that take place in these fibers: conformational change, chain orientation, and crystallinity. The Raman data, in combination with data from X-ray, thermal analysis, density, and birefringence measurements on these same fibers, allow these three events to be separated. On the basis of this analysis, it is now possible to carry out this separation in PET fibers based on Raman spectroscopy alone. Raman polarization data are used to support the arguments.

The vibrational spectrum of poly(ethylene terephthalate) (PET or 2GT) has been extensively studied.[1-18] One of the main reasons for interest in the infrared and Raman spectra of PET is that the spectrum has been characterized as being sensitive to crystallinity. Indeed, such sensitivity is often mentioned in connection with the vibrational spectra of polymers.

In practice, the changes in the infrared and Raman spectra have only rarely been correlated with crystallinity, if we take that to mean the development of long-range, three-dimensional order. However, there have been some correlations with density, thermal analysis, and occasionally with X-ray data.

There have been attempts to explain the changes in the Raman spectrum that occur upon annealing of amorphous samples. These changes, though considered to be related to the development of crystallinity, are explained as being due to conformational changes in either the carbonyl groups or the glycol linkage. Since it is assumed that these conformational changes go hand in hand with crystallinity development, the extension is both logical and reasonable.

Relatively few studies have been carried out on the Raman spectrum of PET fibers or other oriented samples. These have usually focused on the assignment of Raman bands based on polarization.[3,11,19,20] Melveger[11] did show that certain changes in the Raman spectrum did not correlate well with density in the case of fibers and that this seemed to be a problem of orientation complicating the Raman intensities.

What appears to be needed is a study of the effect of conformational change, chain orientation, and crystallinity on the Raman spectrum. It is rarely possible to hold two of these variables constant while the third changes—they are not so independent. But by the use of a combination of varying the fiber and a range of characterization techniques, it should be possible to better understand the spectroscopic changes. As a consequence, this leads to the possibility of a variety of diagnostic techniques and physical understanding which can be derived from the Raman data.

In this paper, we approach this problem as follows: A PET yarn is prepared with a takeup speed of ca. 3300 m/min. This yields what is known as a partially oriented yarn (POY), which is oriented but still amorphous and in which the conformational disorder is great. This yarn is then annealed under a range of annealing conditions so that chain orientation, conformation, and crystallinity result in different combinations. In this way a set of five fibers, the original and four new ones prepared by annealing, is produced. Each of these is characterized by its Raman spectrum and by thermal analysis, birefringence, density, and wide-angle X-ray diffraction. It will be seen that the resulting data show that the Raman spectrum has great potential for separating the kinds of changes which are occurring, and, in the future, for following these changes as they occur. Raman polarization data on single filaments are used to support the analysis, but the basic

† Visiting Professor. Permanent address: Israel Fiber Institute, Jerusalem, Israel.

0024-9297/85/2218-2587$01.50/0

data come from multifilament yarn bundles.

Experimental Section

The PET fibers, without finish or dilustrant, were originally supplied to D. Selivansky[21] by Fiber Industries of Celanese Corp., who kindly provided them to us for this study. The fiber was melt-spun at 288 °C from PET chips of intrinsic viscosity 0.675, with a takeup speed of 3292 m/min. Partially oriented yarns (POY) of 116/33 denier were formed.

The POY was post-processing treated with specific annealing conditions to alter microstructure as follows: 2GT control, original fiber; $2GT_{70}$, annealed with ends free at 70 °C for 60 min; $2GT_{86}$ annealed with ends fixed, 86 °C for 2.5 min; $2GT_{122}$, annealed with ends fixed, 122 °C for 5 min; $2GT_{152}$ annealed with ends fixed, 152 °C for 5 min.

Raman spectra were obtained by using the Jobin-Yvon HG2S Ramanor spectrometer, automated for data collection and reduction with a Data General Nova 2 computer. Spectral slit widths were ca. 1 cm^{-1} for all measurements. Excitation was by a Spectra-Physics Model 165 argon ion laser, operating at 0.25-W power at 488 nm.

For the multifilament spectra, i.e., all but those on which the depolarization ratios were measured, a yarn holder was constructed for the Raman sample chamber which allowed a semirandom orientation of filaments within the bundle to be illuminated by the laser. This is done to effect a scrambling of the filament orientations and assure that only the internal changes within the fibers, and not the sample placement, cause changes in the spectra.

For the single-filament polarization data, just the opposite approach is used. The filament (a few micrometers thick) is carefully aligned with respect to both the incident laser beam polarization and the analyzer. This is done by constructing a rectangular glass frame to which a single filament can be fixed between parallel sides and rotated to enable polarization measurements to be made. Polarization measurements were then made by standard techniques.

Intensities were all taken as peak heights at the relevant wavenumbers given in the figures. Because most of these involved overlapping bands, area measurements are not feasible. Error bars shown in the figures are calculated by assuming that the measured intensities (as total photon counts) have standard deviations that are proportional to the square root of the number of counts. Propagation of errors is then used to calculate the standard deviation of the computed result.

Birefringence and X-ray data were obtained by Selivansky,[21] and details are provided in his thesis. Dumbleton's index[22] of crystallinity was determined from each diffraction pattern. Density was measured by us using a Techne DC-1 density gradient column thermostated at 23 ± 0.1 °C. The method followed was ASTM D 1505-6, and the solvents used were *n*-heptane and CCl_4, producing a density range of 1.28–1.45 g/cm^3.

Thermal analysis was performed by using a Du Pont 1090 thermal analysis system, including the data analysis microprocessor. To minimize microstructural perturbations to the annealed samples, the fibers were not cut into small pieces to fill the sample pan. Instead, the yarns were coiled about a polyethylene hollow tube of ca. 2-mm i.d. with sufficient flexibility to slide the coil formed off the tube and into the DSC hermetic pan to be sealed. In this analysis, the fibers are thus free to shrink. The heating rate (10 °C min) and time/point (0.2 s) averaging were identical for all scans.

Results

Raman Spectra of the Five Fibers. Five fibers have been studied. The first, control fiber, is a POY prepared with a takeup speed of 3292 m/min. This sample was annealed with the ends free at a temperature close to the glass transition, yielding a fiber referred to as $2GT_{70}$, which had shrunk considerably and had a greatly reduced orientation. The original fiber was also annealed with the ends held fixed at three different temperatures, yielding the samples $2GT_{86}$, $2GT_{122}$, and $2GT_{152}$.

Figures 1–3 show the Raman spectra of these five samples. While previous papers have suggested that there are

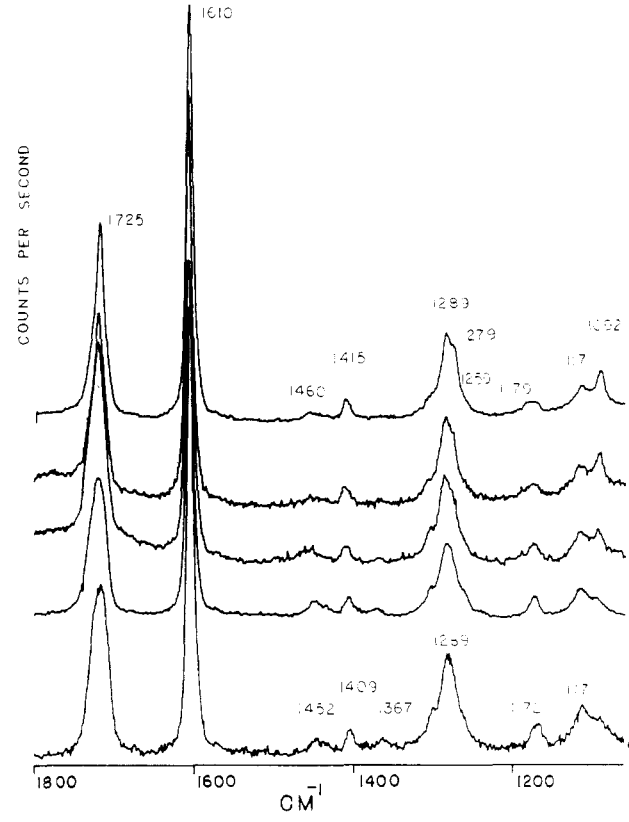

Figure 1. Raman spectra of the five fibers in the 1040–1800 cm^{-1} region: (a) 2GT; (b) GT_{70}; (c) $2GT_{86}$; (d) $2GT_{122}$; (e) $2GT_{152}$.

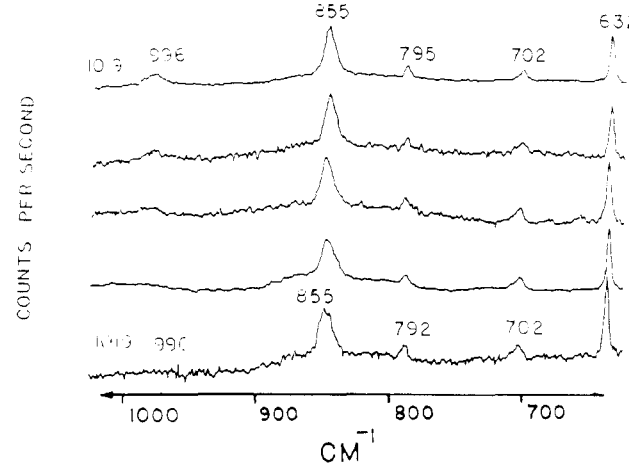

Figure 2. Raman spectra of the five fibers in the 620–1040 cm^{-1} region: (a) 2GT; (b) $2GT_{70}$; (c) $2GT_{86}$; (d) $2GT_{122}$; (e) $2GT_{152}$.

between two and five changes in the spectrum with annealing, it can be seen from these data that in the fiber samples virtually every band in the spectrum changes under at least some of the annealing conditions. Put another way, each of these five fibers have Raman spectra that are distinct in at least one spectroscopic region.

Because these changes are used to understand morphological changes in what follows, it is useful to establish quantities that are good spectroscopic parameters characterizing each change. Such parameters should be independent of both the concentration of scatterers and any multiple scattering due to refractive index discontinuities. For this purpose we use the following changes:

1. The two most established changes in the spectra are the width of the carbonyl stretching vibration and the growth of the new band at 1092 cm^{-1}. For the former we used the full width at half height and for the latter the

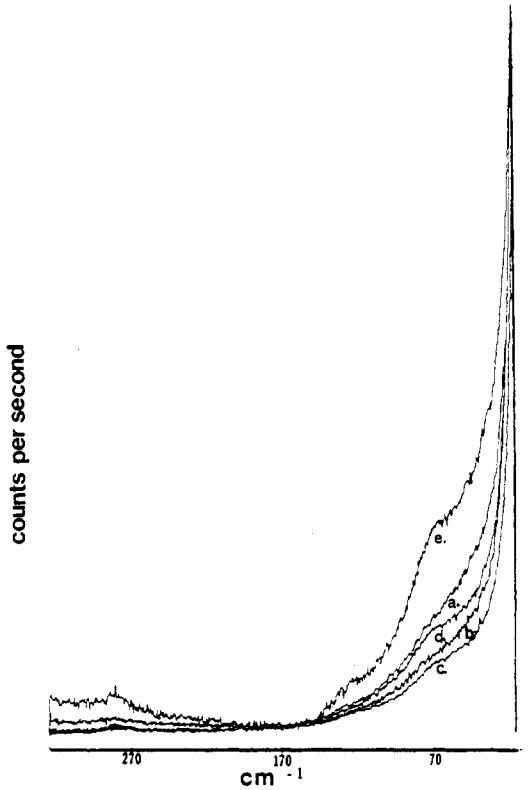

Figure 3. Raman spectra of the five fibers in the 20–300 cm^{-1} region: (a) 2GT; (b) $2GT_{70}$; (c) $2GT_{86}$; (d) $2GT_{122}$; (e) $2GT_{152}$.

ratio of the intensity at 1092 cm^{-1} to that at 1117 cm^{-1}. Melveger[11] had previously used the ratio of 1092/632 cm^{-1} intensity, but this causes problems because, as will be described below, the 632-cm^{-1} band changes in other, complex ways itself.

2. There is a weak band at 1452 cm^{-1} in the control sample that shifts its peak intensity to 1460 cm^{-1} in the most highly annealed samples. To characterize this change, the ratio of intensities at these two wavenumbers is used. Other intensity ratios based on a shift are 1415/1409, 1279/1259, 996/1019, 795/792, and 282/273. Each of these pairs seems to be coupled during the annealing process.

3. A similar change occurs in the region of 1172–1179 cm^{-1}, but the bands are weak, broad, and sufficiently overlapped that particularly for samples of intermediate crystallinity it is not possible to locate either the frequency maxima or the intensities very well. For this reason, we have somewhat arbitrarily characterized this change by measurement of the half width of the overall feature.

4. Two other bands, the well-isolated, sharp band at 632 cm^{-1} and the peak at 855 cm^{-1}, change in relative intensity during the annealing process, but there is no obvious neighbor band that is coupled to the band in question. In these cases the relative intensity of the band to that at 1289 cm^{-1} is used. The 1289-cm^{-1} band appears to be of rather constant intensity, although with everything else changing, including features in the wings of this band, it is rather hard to say that this intensity is really constant. The 1610-cm^{-1} band is also nearly constant in intensity and half width, but its intensity is so large that its use as the denominator in an intensity ratio produces serious roundoff errors.

5. The low frequency region data show major changes with annealing. New bands at 73 and 129 cm^{-1} grow in, and a broad low-frequency mode centered near 30 cm^{-1} disappears. Results in this region have been presented and discussed in more detail in a separate paper.[23] The spectra as presented in Figure 3 are already normalized to the intensity at 20 cm^{-1}. Therefore, in examining the changes in the spectra, we use the intensity at 73 cm^{-1} directly. This is obtained, however, from a tangent to the sloping background rather than from the base line.

It is worth emphasizing that while the intensity of a band in the Raman spectrum should be proportional to concentration, these parameters, selected somewhat arbitrarily, need not be directly proportional to concentration. However, as we will see when they are examined in comparison to each other and to other data on these samples (e.g., thermal analysis, density, birefringence, etc.), the results can be quite enlightening as to the origin of the changes observed. Thus we do not necessarily expect or find linear behavior when various spectroscopic changes are plotted against each other or against concentration, but we do look for trends or changes in the same direction, albeit with a sometimes complex proportionality relationship.

Table I
Depolarization Ratios for Fibers 2GT and $2GT_{70}$

wavenumber, cm^{-1}	2GT	$2GT_{70}$
272	1.25	0.70
632	1.20	0.77
702	0.008	0.01
792	1.7	1.2
855	0.08	0.07
1117	0.16	0.09
1289	0.01	0.01
1367	1.0	0.67
1409	0.02	0.01
1452	0.83	0.60
1612	1.10	1.0
1725	0.27	0.17

Table II
Density, X-ray, and Birefringence Data on Fibers

sample	density, g/cm^3	X-ray, Dumbleton index	birefringence
2GT	1.3446	0	0.0486
$2GT_{70}$	1.3428	0	0.0292
$2GT_{86}$	1.3500	0.12	0.0544
$2GT_{122}$	1.3759	0.50	0.1053
$2GT_{152}$	1.3870	0.60	0.1172

Polarization Data on Two Single Filaments. To aid in the understanding of the role of orientation in the Raman data, the polarization spectra of single filaments have been examined. Figure 4 shows the Raman spectrum of an oriented filament of the control sample in two positions of the analyzer. Figure 5 shows the same experiment on sample $2GT_{70}$. Note that most of the bands in the spectrum are highly polarized; that is, their intensities are much less when the analyzer selects for the zx direction than for the zz. This is as expected for a sample of very low symmetry, such as the highly amorphous PET. However, for the 632-cm^{-1} band this is not the case. It is seen to be more intense in I_{zx} than in I_{zz} for the control and less intense for $2GT_{70}$. This change can only occur if there is a substantial change in orientation that affects the Raman spectrum. Similar changes affect some of the other bands in the spectrum (273, 792, 1367, 1452 cm^{-1}). The low intensity of these other bands makes the ratios subject to much higher uncertainties, however. The importance of this result will become clear when we discuss the behavior of the intensity of the 632-cm^{-1} band in the five samples. The values of the depolarization ratios for the two fibers are given in Table I.

Density, X-ray, and Birefringence Data. Table II summarizes data from these three additional techniques

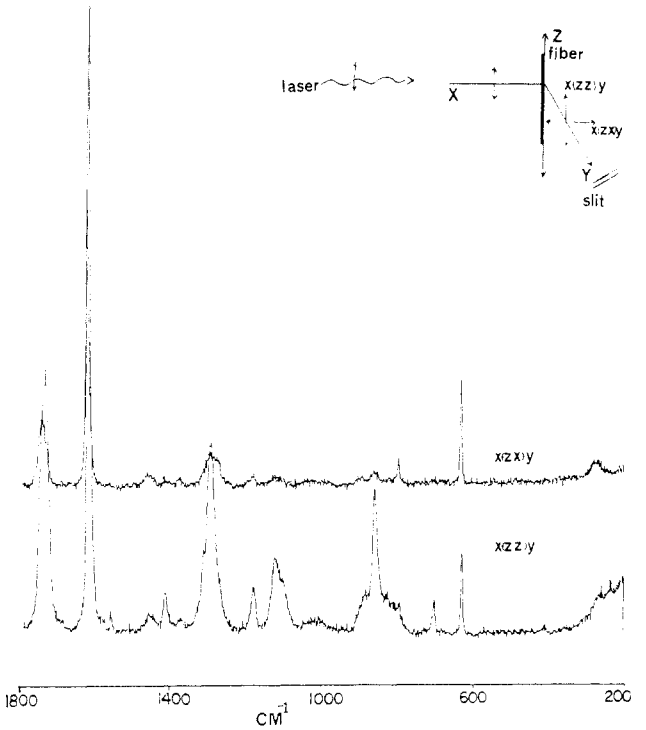

Figure 4. Raman polarization spectra of an oriented filament of 2GT sample fiber: (top) spectrum $x(zx)y$, in which the analyzer is perpendicular to the incident polarization; (bottom) spectrum $x(zz)y$, in which the analyzer is parallel to incident polarization.

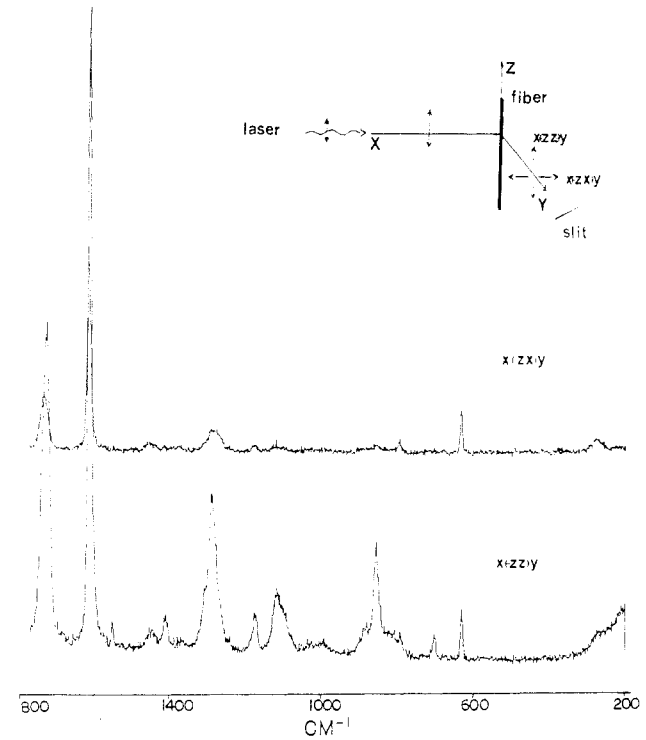

Figure 5. Raman polarization spectra of fiber sample $2GT_{70}$. Analyzer as indicated on the spectra.

on the same samples. Density data are from our own measurements, while the X-ray and birefringence data are from Selivansky.[21] Even a cursory examination of these data indicates that they are not following the annealing process with the same response function. This complexity in the observations will be discussed in the following sections.

Thermal Analysis. DSC data for the five samples are shown in Figure 6 and summarized in Table III. It is clear

Table III
Thermal Analysis Data on Fibers

sample	T_g, °C	T_{cr}	ΔH_{cr}, J/g	T_{lm}	T_m	ΔH_f, J/g
2GT	60, 73	99	8.2	86	257.1	28.9
$2GT_{70}$	79	104	11.5	85	257.8	29.1
$2GT_{86}$	80	102	3.8	92	254.6, 257	37.1
$2GT_{122}$				130	251.5, 257	41.1
$2GT_{152}$				180	256.9	38.8

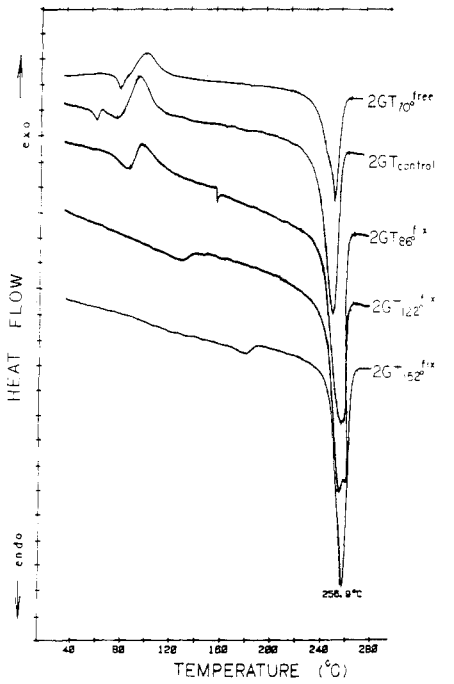

Figure 6. DSC data on the five fiber samples.

that each sample has a different thermal behavior in the DSC. The control POY shows two T_g values, 60 and 73 °C, and two endotherms in addition to the main melting. The second endotherm, at 86 °C, is followed by an exothermic area, and finally the main melting endotherm is seen.

The two samples annealed at low temperature show only one T_g value and one low endothermic peak followed by an exotherm. The remaining two samples, annealed at the higher temperatures, show neither a glass transition nor an exotherm, and the low-melting endotherm moves to higher temperatures. The $2GT_{122}$ sample and, to a lesser extent, the $2GT_{86}$ sample show a split of the main endotherm, a fact that has been observed in the past for certain crystalline samples.[24]

The heats of fusion and crystallization were calculated as the areas between the DSC trace and a base line constructed from the beginning of the lower melting peak above the T_g to the end of the high melting peak in the thermogram, with normalization for sample weight. The values of ΔH_f in Table III are the net endothermic areas after subtraction of the crystallization exothermic areas. This method of calculation provides information on the properties of the samples before the thermal analysis.

Discussion

When partially oriented PET samples are annealed, several things can happen. The relative amounts of amorphous and crystalline phases change. This is both preceded and accompanied by conformational change within the chains. The orientation of the amorphous and crystalline phases also changes.

When Raman spectra of bulk, unoriented PET samples are studied as a function of annealing, there are relatively

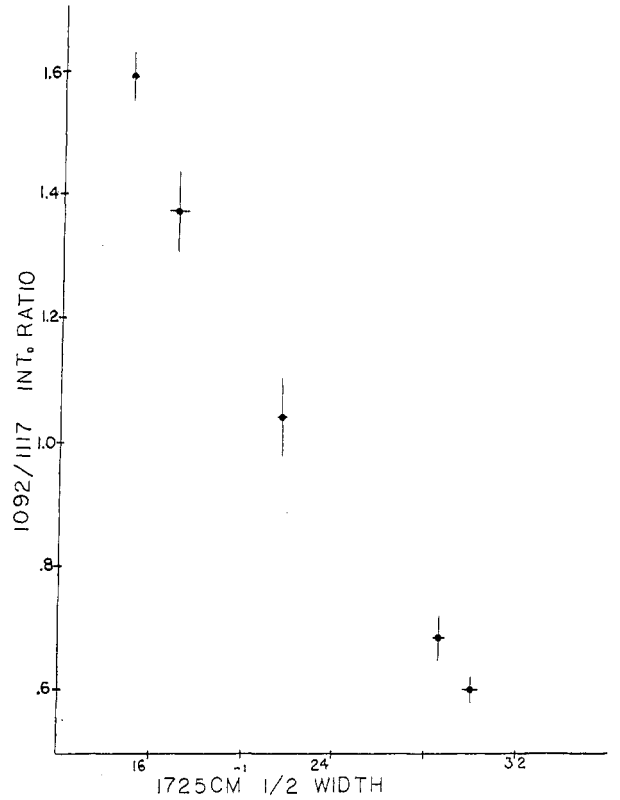

Figure 7. Correlation of the intensity ratio I_{1092}/I_{1117} with the half bandwidth of the carbonyl stretching mode. Error bars are calculated as described in the Experimental Section.

few changes. When oriented samples are studied, as in this paper, almost every band in the spectrum changes. This increased sensitivity of the spectrum indicates that it may be possible, by the use of Raman data, to separate the different things which are happening.

This analysis is approached as follows: In the first part of the Discussion we present (internal) correlations between the different spectroscopic changes. This allows one to examine whether these spectroscopic changes seem to be measuring the same molecular phenomena. These correlations will in fact show that a number of different phenomena are being observed.

To assign the spectroscopic changes to particular events, other data are used. These are called external correlations. Most of the external data are straightforwardly interpreted and used. The polarization data, which support the interpretation, are dealt with separately.

In the final part of the Discussion, a unified picture of the changes on annealing is presented, taking into account the data from Raman spectroscopy, density, X-ray, birefringence, and the rather complex thermal analysis results.

Internal Correlations. Figure 7 shows a plot of the intensity ratio at two wavenumbers, 1092/1117, vs. the half bandwidth of the carbonyl stretching mode at 1725 cm^{-1}. There is a very nearly linear relationship here, with a correlation coefficient >0.99 for the least-squares straight line. It must be assumed that these two spectroscopic changes measure the same molecular phenomenon. This sort of correlation is also found when the intensity ratio 1452/1460 cm^{-1} is plotted vs. carbonyl half width and for the intensity ratio 1415/1409 vs. carbonyl half width (Figure 8). These four changes form a first group.

It has previously been suggested[11] that the 1092-cm^{-1}band did not correlate with carbonyl half width for oriented samples. This is true of the intensity ratio 1092/632, used previously, as the 632-cm^{-1} band behaves quite differently in oriented samples only.

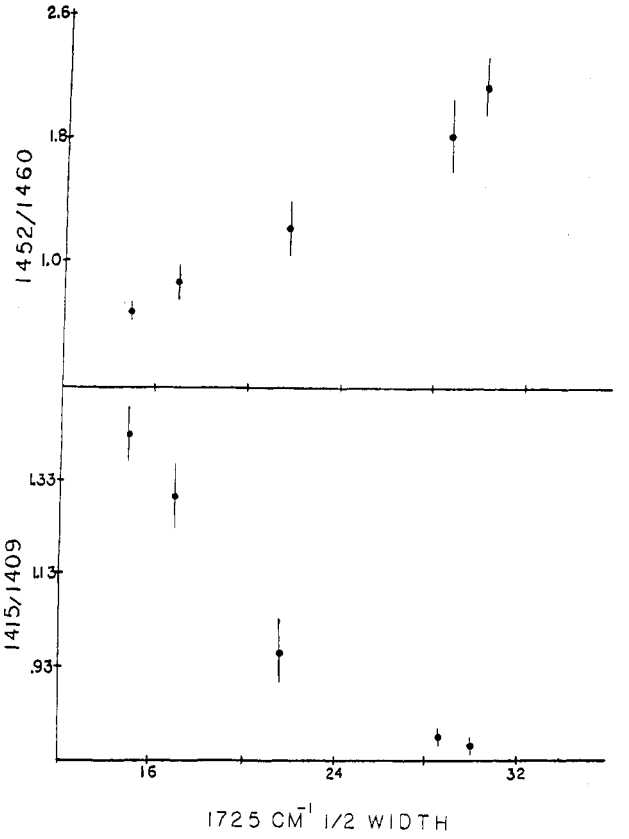

Figure 8. Correlation of intensity ratios of 1452/1460 and 1415/1409 with half bandwidth of the carbonyl stretching mode.

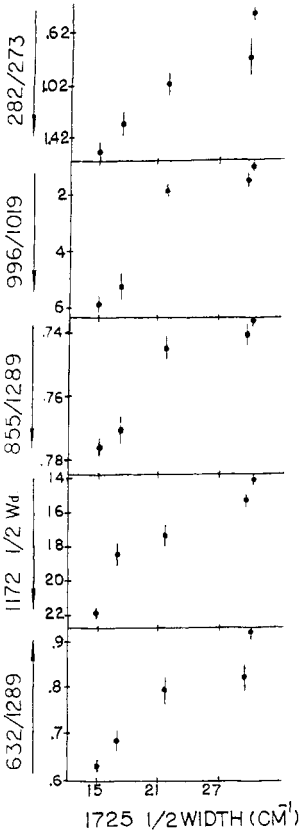

Figure 9. Intensity ratios and bandwidth for five sets of bands correlated with half bandwidth of the carbonyl stretching mode.

This point is clearly seen in Figure 9, which plots the 632-cm^{-1} intensity (relative to 1289 cm^{-1}, as described above) vs. $\Delta\nu_{1/2}$ (1725). This strange dependence on annealing is also found for other cases shown in Figure 9,

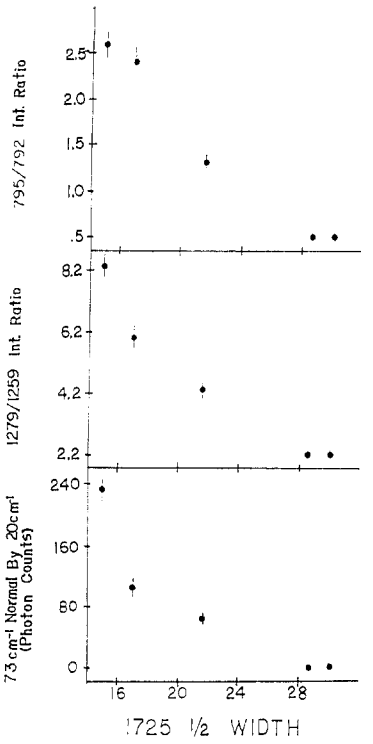

Figure 10. Intensity ratios for three sets of bands correlated with the half bandwidth of the carbonyl stretching vibration.

namely the 1172/1179 half width, the 855-cm^{-1} relative intensity, and the 996/1019 and 282/273 cm^{-1} ratios. These curves may be best-characterized by noting the sharp discontinuity between the two more amorphous samples and the three more crystalline ones. This is the second group.

The third and final group is the 73-cm^{-1} intensity and the intensity ratios 1279/1259 cm^{-1} and 795/792 cm^{-1} plotted vs. carbonyl half width. This is seen in Figure 10. The essential change here is that the samples 2GT and $2GT_{70}$ give the same value in each case. It may be noted that the change in these two samples for the 1415/1409 cm^{-1} ratio is very small, and this may fall into group three instead of group one.

These groupings would be of only passing interest if it were not for a striking fact: When viewed together with the vibrational analysis of PET by Boerio et al.[13] one sees that they also represent groupings of molecular vibrational motions.

The most clear-cut of these is group 2, which is almost completely modes that are localized to the phenyl rings. These modes are not sensitive to annealing in the bulk samples of PET, and the sensitivity only develops in the oriented materials. The rigidity of the phenyl rings thus allows one to follow orientation independent of conformational change.

The first group is the modes that, by contrast, are most sensitive to conformational change. They involve the stretching and out-of-plane deformation modes of the glycol and ester linkage. Any conformational change in this linkage must result in a change in the potential energy distribution of these modes, as the relevant bond angles are changing. The carbonyl stretching mode falls into this group by a different mechanism. It is still the C=O stretch, but change in conformation alters its force constant through interaction with the ring π system and narrows the distribution of environments.

Group 3 is small but essentially consists of two in-plane motions of the ester linkage and the low-frequency mode, which is probably a torsional mode. This is an important group because it seems to be insensitive to changes that are due to orientation only.

To summarize, the changes observed in the spectra of the five fibers are neither of one sort nor random, but can be classified into three distinct groups. These groups are also approximate groupings of the vibrational modes. In the following sections, the spectrum will be discussed in terms of these groups and other data on the fibers.

Supporting Data from Polarization. Spectra of the oriented single filaments of 2GT and $2GT_{70}$ support this view. Several of the bands in the spectrum are highly polarized for both fibers. However, the 632-cm^{-1} band actually shows a depolarization ratio of 1.20 in 2GT, a value that can only be obtained for a sample such as this one in the case of significant orientation. When the sample is annealed to $2GT_{70}$, this ratio drops to 0.77, which, within experimental error, is the value expected for a depolarized band in an unoriented sample, as has already been reported for bulk samples of amorphous PET.[19] Once again we see the sensitivity of this ring mode to orientation. There are several other weak bands that also have depolarization ratios greater than 1 in 2GT. In each case the ratios decrease in $2GT_{70}$, though not to values as low as would be expected for an unoriented bulk sample. No such anomalously high ratios are found for bulk PET.[19,25]

Many other modes also change their depolarization ratios in this way between these two fiber samples. The general observation is that almost every band in the spectrum has a lower depolarization ratio in $2GT_{70}$ than in the original 2GT. Given the lack of symmetry in these samples this decrease is expected. It is consistent with a substantial decrease in chain orientation without any increase in local symmetry.

External Correlations. We now consider the phenomena on which each of these spectroscopic groups is reporting. To separate these, resort is made to data on the five fibers from other techniques.

Group 1 is the carbonyl stretching mode, the 1092/1117 pair, the CH_2 deformations (1452–1460), and possibly the 1415–1409 pair. This group is only changing due to conformational change in the glycol linkage. The conformational change begins at the ends with the carbonyl groups and extends to the center of the linkage with the gauche–trans isomerization.

If one examines the data from this group, it is clear that it really only correlates with conformational change and not with anything else. This is important because these are usually thought of as the "crystallinity" bands.

There is, however, a reasonable correlation between four of the fibers in their group 1 spectra and density. This is seen in Figure 11. This was previously noted for the C=O half width by Melveger.[11] Figure 11 shows that the $2GT_{86}$ sample deviates from the nearly linear relationship. Its density is lower than expected for the carbonyl half width it exhibits. This is explainable in light of the small crystals that are probably present in this sample. They disrupt the order of the amorphous phase, yet are not sufficiently large or numerous to pack efficiently.

Group 2 modes are all associated with the phenyl ring. When one compares their behavior with that of group 1 modes (e.g., see Figure 9), the behavior is very nonlinear. External correlations of group 2 data with overall birefringence resolves this. This is shown for the 632-cm^{-1} band in Figure 12. A similar near-linear plot is obtained for the band at 855 cm^{-1} and for the pairs at 996–1019, 1172–1179, and 282–273 cm^{-1}. These ring modes are thus sensitive to orientation only, and this is what is monitored by birefringence.

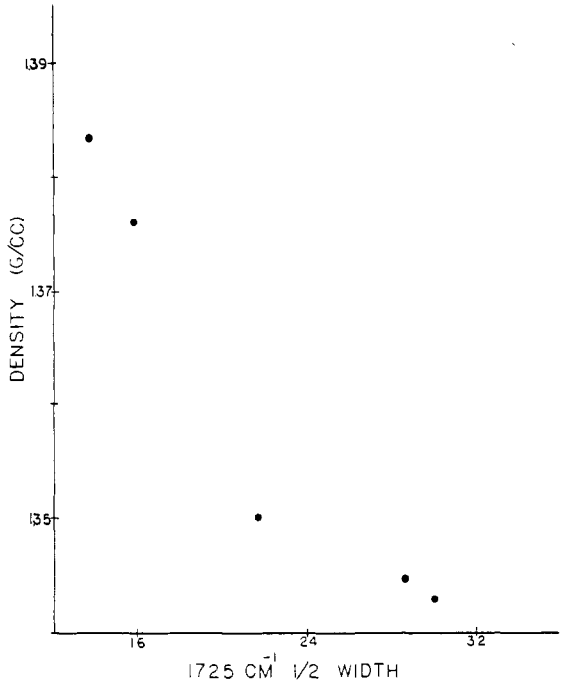

Figure 11. Correlation between the density of the five fibers and the half bandwidth of the carbonyl stretching mode.

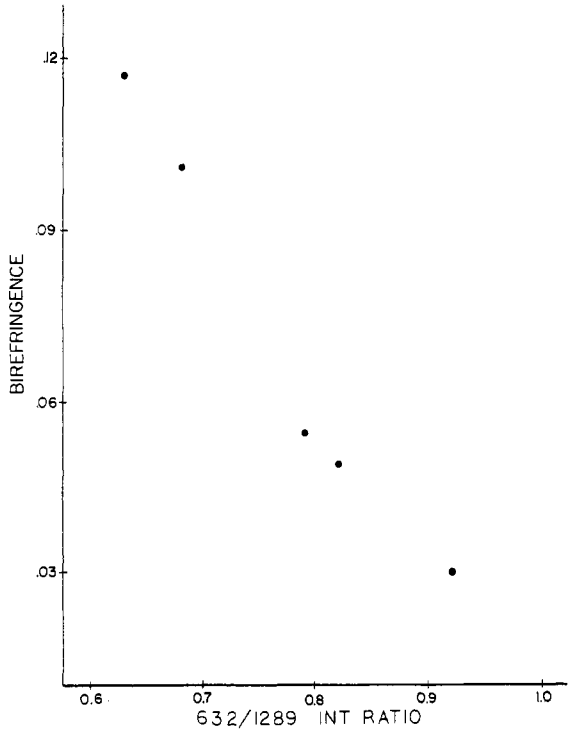

Figure 12. Correlation between the birefringence measurements of the five fibers and the 632/1289 intensity ratio.

The modes in group 3 are unchanged for the annealing from 2GT to $2GT_{70}$, but grow when annealing at higher temperatures with the ends fixed. This then is the behavior that should relate to crystallinity, and it does. Figure 13 shows the correlation of the 795/792 cm^{-1} intensity with a crystallinity index developed from wide-angle X-ray scattering. The X-ray data, like the spectroscopic data in group 3, show no change for 2GT to $2GT_{70}$ and then increase steadily with the other three samples.

The 73-cm^{-1} band is readily understood in this context. Whether an internal or external mode (probably the former), it is nonetheless connected to long-range order. In a separate paper, we will show[26] that this mode only begins

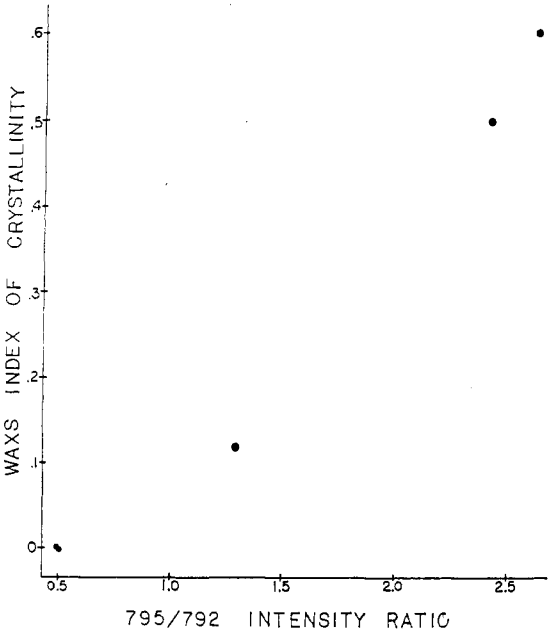

Figure 13. Correlation of the WAXS Dumbleton's crystallinity index with the 795/792 intensity ratio.

to develop in the later stages of annealing after substantial change has already occurred in the carbonyl and glycol unit modes. The other modes in this group, for the most part describable as in-plane vibrations of the linkage, seem to be most sensitive to interchain vibrations. These then are the true "crystallinity" bands in the Raman spectrum of PET fibers.

Changes on Annealing. It can be seen from the foregoing that the X-ray crystallinity index becomes significant only upon annealing at 86 °C, while the low amount of small crystallites in the 2GT and $2GT_{70}$ samples are undetected by this technique. The X-ray crystallinity index of 0.12 obtained for $2GT_{86}$ is much lower than the value that would correspond to the relatively high heat of fusion found in the DSC measurements.

The birefringence measurements indicate an orientation factor of 0.215 for 2GT, calculated by assuming, following Konda et al.,[27] that the intrinsic birefringence of the crystalline regions of PET is equal to that of the amorphous regions, so that the value of 0.212 can be used for the whole fiber.

Annealing at 70 °C with ends free brings about several changes in the amorphous regions: First, the frozen-in local stresses of the glassy 2GT are released. It is to these stresses that the lower T_g value and the endotherm following it are attributed. Boyer[28] believed that the double T_g is associated with two differently ordered amorphous phases. Cuculo et al.[30] suggest that the secondary low T_g value is due to a transition in local order during stretching. Annealing at 70 °C with ends free brings about the disappearance of the low T_g and the small endothermic peak following it. These changes will manifest thermselves by changes in local conformation of functional groups, as evidenced by changes in the group 1 Raman bands.

Second, during this annealing period the oriented segments of the chains in the amorphous regions of the POY undergo a disorientation. This is an endothermic event that reflects a change in the orientational part of the entropy of fusion.[31] This decrease in orientation accompanied by considerable shrinkage of the fiber manifests itself in the sharp decrease in birefringence and in changes in the Raman bands of group 2 linked to orientation.

Third, the cold crystallization temperature T_{cr} increases between 2GT and $2GT_{70}$ from 99 to 104.4 °C. When an-

nealing is done to produce $2GT_{86}$, T_{cr} decreases to 102.4 °C. There are two ways of approaching this. The decrease in orientation when $2GT_{70}$ is produced makes the chains, now containing a larger percentage of gauche conformers, more difficult to align and pack into a crystalline lattice. Alternatively, the increase in the temperature of annealing is found to increase T_{cr}, presumably due to the additional disordering effect stemming from higher mobility at the higher temperatures.[32] The fact that T_{cr} decreased from $2GT_{70}$ to $2GT_{86}$ implies that the stress developed during the taut annealing at 86 °C must have preserved the orientation of the amorphous regions, as was also found from the birefringence measurements. This predominated over the opposing effect of the temperature. There is also a great difference in the annealing times at the two temperatures, and it is difficult to equate these in any way because of the proximity to the glass transition. The increase in orientation observed by thermal analysis and birefringence manifests itself in the low-frequency region[23] and in the Raman bands in group 2.

The changes occurring upon annealing to give $2GT_{86}$ are more profound than those for $2GT_{70}$. The relatively high heat of fusion indicates a considerable degree of crystallinity which is corroborated by the low exothermic heat of crystallization.

While the Raman bands of groups 1 and 3 also indicate a significant degree of crystallinity in sample $2GT_{86}$ compared to 2GT, the density, as seen in Figure 11, is smaller than expected. This would indicate that when annealing at constant length, new nuclei and small, imperfect crystals were formed at random due to the mobility imparted to chains by the rapid decrease in stress and the lack of shrinkage. Parts of the amorphous chains necessarily become extended, which must be accompanied by the formation of voids in the structure, hence the low density of this sample. The short time and relatively low temperature of annealing must have produced relatively small crystallites, only poorly detected by the WAXS measurements.

The changes from the control to $2GT_{86}$ are thus seen in all three groups of Raman bands. This is also the case for the samples $2GT_{122}$ and $2GT_{152}$, which crystallized to a relatively high amount, as evidenced by the WAXS, density, and Raman data. These samples exhibited neither a glass transition nor a cold crystallization. The temperature of the low-melting endotherm increased upon increasing annealing temperature, and the values are comparable to those reported in the literature.[33-37]

The low-temperature endotherm, which can appear immediately after the glass transition,[38] has been reported for PET in the form of fibers,[33,34] and isotropic,[35] oriented,[36] and unoriented films. It reflects the distribution of crystallite sizes and is believed to be an ongoing melting and recrystallization of the small crystallites into more perfect crystals.

The possibility of two crystalline phases or two types of crystals, e.g., extended and folded,[24] has also been suggested from the thermal analysis data. The low-temperature endotherm may affect the relative amounts of these two phases and their appearance as a split peak in the main melting endotherm. This splitting is clearly seen in our $2GT_{122}$ sample and is also present in the $2GT_{86}$ sample. However, it may not manifest itself in the Raman data because these data are taken before the sample has undergone the low-endotherm transition.

It is this very complex recrystallization and melting process, encompassing conformational change, orientational change, and disorder, that makes it impossible to select particular values of heats from the DSC data to compare with individual Raman bands.

Conclusion

The Raman data on this set of five fibers indicate that it is possible, by the use of this technique alone, to separate conformational change, orientation of chains, and crystallinity. Other techniques measure one of these properties (birefringence, X-ray) or a mixture of them (DSC, density). The data also point the way to further studies on fiber annealing using Raman spectroscopy. Such work is in progress in our laboratory and will be reported shortly.

Acknowledgment. This work was supported by the Polymers Program of the National Science Foundation, Grant DMR-8304220. We are grateful to Dr. D. Selivansky for helpful discussions and cooperation.

References and Notes

(1) Miyake, A. *J. Polym. Sci.* **1959**, *38*, 479.
(2) Liang, C. Y.; Krimm, S. *J. Mol. Spectrosc.* **1959**, *3*, 554.
(3) Farrow, G.; Ward, I. M. *Polymer* **1960**, *1*, 330.
(4) Manley, T. R.; Williams, D. A. *Polymer* **1969**, *10*, 339.
(5) Statton, W. O.; Koenig, J. L.; Hannon, M. *J. Appl. Phys.* **1970**, *41*, 4290.
(6) Prevorsek, D. C.; Sibilia, J. P. *J. Macromol. Sci., Phys.* **1971**, *5*, 617.
(7) Sibilia, J. P.; Harget, P. J.; Tripak, G. A. *Polym. Prepr. (Am. Chem. Soc., Div. Polym. Chem.)* **1974**, *15*, 660.
(8) Cunningham, A.; Ward, I. M.; Willis, H. A.; Zichy, J. V. *Polymer* **1974**, *15*, 749.
(9) D'Esposito, L.; Koenig, J. L. *J. Polym. Sci., Polym. Phys. Ed.* **1976**, *14*, 1971.
(10) McGraw, G. E. In "Polymer Characterization, Interdisciplinary Approach"; Craver C. D., Ed.; Plenum: New York, 1971.
(11) Melveger, A. J. *J. Polym. Sci., Polym. Phys. Ed.* **1972**, *10*, 317.
(12) Bahl, S. K.; Cornell, D. D.; Boerio, F. J.; McGraw, G. E. *J. Polym. Sci., Polym Lett. Ed.* **1974**, *12*, 13.
(13) Boerio, F. J.; Bahl, S. K.; McGraw, G. E. *J. Polym. Sci., Polym. Phys. Ed.* **1976**, *14*, 1029.
(14) Purvis, J.; Bower, D. I. *J. Polym. Sci., Polym. Phys. Ed.* **1976**, *14*, 1461.
(15) Tonelli, A. E.; *J. Polym. Sci., Polym. Lett. Ed.* **1973**, *11*, 441.
(16) Venkatesh, G. M.; Bose, P. J.; Shah, R. V.; Dweltz, N. E. *J. Appl. Polym. Sci.* **1978**, *22*, 2357.
(17) Stokr, J.; Schneider, B.; Joskocilova, D.; Lowy, J.; Sedlacek, P. *Polymer*, **1982**, *23*, 714.
(18) Ward, I. M. *Polymer* **1977**, *18*, 327.
(19) Purvis, J.; Bower, D. I.; Ward, I. M. *Polymer* **1973**, *14*, 398.
(20) Ward, I. M. *J. Polym. Sci., Polym. Symp.* **1977**, *58*, 1.
(21) Selivansky, D. Ph.D. Thesis, North Carolina State University, 1983.
(22) Dumbleton, J. H.; Bowels, B. B. *J. Polym. Sci., Polym. Phys. Ed.* **1966**, *6*, 951.
(23) DeBlase, F. J.; McKelvy, M. L.; Lewin, M.; Bulkin, B. J. *J. Polym. Sci., Polym. Lett. Ed.* **1985**, *23*, 109.
(24) Roberts, R. C. *J. Polym. Sci., Part B* **1970**, *8*, 381.
(25) McKelvy, M. L. Ph.D. Thesis, Polytechnic Institute of New York, 1985.
(26) Bulkin, B. J.; McKelvy, M. L.; Lewin, M., unpublished data.
(27) Konda, A.; Nose, K.; Ishikawa, H. *J. Polym. Sci., Polym. Phys. Ed.* **1976**, *14*, 1495.
(28) Boyer, R. F. *J. Polym. Sci., Polym. Symp.* **1975**, *56*, 189.
(29) Selivansky, D.; Lewin, M. *J. Appl. Polym. Sci.* **1982**, *27*, 2337.
(30) Cuculo, J. A.; Chao, W.; Gallant, A. R.; George, T. W. *Appl. Polym. Symp.* **1975**, *27*, 193.
(31) Wunderlich, B. "Macromolecular Physics"; Academic Press: New York, 1980; Vol. 3.
(32) Sun, T.; Pereira, J.; Porter, R. *J. Polym. Sci., Polym. Phys. Ed.* **1984**, *22*, 1163.
(33) Jaffe, M. In "Thermal Characterization of Polymeric Materials"; Turi, E. A., Ed.; Academic Press: New York, 1981.
(34) Oswald, H. J.; Turi, E. A.; Harget, P. J.; Khanna, Y. P. *J. Macromol. Sci., Phys.* **1977**, *13*, 231.
(35) Roberts, R. C. *Polymer* **1969**, *10*, 112.
(36) Alfonso, G. C.; Pedemonte, E.; Ponzetti, J. *Polymer* **1979**, *10*, 104.
(37) Lin, S. B.; Koenig, J. L. *J. Polym. Sci., Polym. Symp.* **1983**, *71*, 121.
(38) Wunderlich, B.; Grebowicz, J. *Adv. Polym. Sci.* **1984**, *60*, 1.